

# Performances of 2r16APSK and DVB-S2 16APSK Modulations over a Two-Link Satellite Channel

Dayan Adionel Guimarães

**Abstract**—In this paper, the 2r16APSK modulation is contrasted with the 16APSK modulation adopted in the digital video broadcast standard, the DVB-S2, aiming at verifying if the 2r16APSK can be considered an alternative choice for the DVB-S2 and other alike communication systems when subjected to nonlinear distortions. To this end, the performances of both modulations are assessed in terms of the metrics: bit error rate (BER), constellation figure of merit (CFM), peak-to-average power ratio (PAPR), total degradation (TD) versus input back-off (IBO), and spectral regrowth, when the transmitted signal goes through a two-link satellite channel under memoryless nonlinear distortion produced by a traveling wave tube amplifier (TWTA), which is described by the Saleh model. The results show that the 2r16APSK modulation is indeed an alternative choice.

**Keywords**—AM/AM, AM/PM, digital modulation, DVB-S2, nonlinear amplifier, TWTA, 2r16APSK, 16APSK.

## I. INTRODUCTION

**T**YPICAL Earth-satellite-Earth communication systems comprise an Earth station transmitting towards the satellite over the up-link channel, multiple satellite-located repeaters, usually referred to as transponders, and a down-link transmission from the satellite back to the Earth, aiming another Earth station or other receivers located in the satellite's coverage footprint [1].

The main transponder component device of interest here, from the perspective of adding distortion to the transmitted signal, is the satellite's power amplifier. Examples of such device are the traveling wave tube amplifier (TWTA) and the solid state power amplifier (SSPA) [2].

A common characteristic of TWTAs and SSPAs is nonlinearity in signal amplitude and, possibly, in signal phase as well, which may cause amplitude-to-amplitude (AM-to-AM) distortion and amplitude-to-phase (AM-to-PM) distortion, respectively.

AM-to-AM distortion is associated with the nonlinear magnitude transfer characteristic of the amplifier as a function of input signal magnitude. Analogously, AM-to-PM distortion is associated with the nonlinear phase transfer characteristic of the amplifier as a function of input signal magnitude.

The AM-to-AM nonlinear transfer characteristic also causes spectral regrowth, yielding adjacent transponder interference.

Dayan Adionel Guimarães is with the National Institute of Telecommunications (Inatel), PO Box 05, 37540-000 Santa Rita do Sapucaí - MG - Brazil (Tel:+55 (35) 3471 9227, Fax:+55 (35) 3471 9314, e-mail: dayan@inatel.br)

This work was supported in part by RNP, with resources from MCTIC, Grant No. No 01245.010604/2020-14, under the 6G Mobile Communications Systems project of the Radiocommunication Reference Center (*Centro de Referência em Radiocomunicações*, CRR) of Inatel, Brazil, and in part by CNPq and FAPEMIG. DOI: 10.14209/jcis.2022.14.

AM-to-PM nonlinearity causes nonuniform signal constellation rotation, yielding additional bit errors [1].

There are digital modulations that perform better than others under AM-to-AM and AM-to-PM distortions, which is the case of some amplitude-phase shift keying (APSK) modulations. The vast family of APSK modulations are those in which the amplitude and the phase of the carrier are varied according to the data bits [3]. The sub-family of APSK modulations considered herein is the one having the constellation symbols lying on two concentric rings. Two modulations were selected from this sub-family for the analyses presented in this paper: the 2r16APSK modulation proposed in [4], and the 16APSK modulation adopted in the second generation satellite Digital Video Broadcasting (DVB-S2) standard [5].

In the case of the 16APSK constellation, 4 symbols are placed equally-spaced on the inner ring and the remaining 12 symbols are placed equally-spaced on the outer ring [5]. There are six possible radius ratios for the 16APSK constellation rings, as specified in [5, Table 9], designed to improve performance in typical satellite channels.

In the case of the 2r16APSK, 8 symbols are placed equally-spaced on the inner ring and the remaining 8 symbols are placed equally-spaced on the outer ring [4]. A single radius ratio is specified for the 2r16APSK constellation, whose value has been optimized to minimize the bit error rate over an additive white Gaussian noise (AWGN) channel.

Additional information about the 2r16APSK and the 16APSK modulations are given in Section II. Detailed information about these modulations can be found, for instance, in [4] and [5], respectively.

### A. Related work

In [4], the modulations two-radii 8-ary and 16-ary APSK, respectively called 2r8APSK and 2r16APSK, were proposed as alternatives to 8-ary phase-shift keying (8PSK) and square 16-ary quadrature amplitude modulation (16QAM), in this order. It has been shown in [4] that the 2r8APSK achieves higher power efficiency than the 8PSK, at the cost of a higher peak-to-average power ratio and a slightly more complex receiver. The 2r16APSK yields lower peak-to-average power ratio than the 16QAM, with roughly the same receiver complexity, but at the cost of a slightly lower power efficiency.

The design criteria of the 2r8APSK and the 2r16APSK constellations was the minimization of the bit error probability achieved by a maximum-likelihood receiver over the AWGN channel. Comparisons with other APSK-based modulations were also made in [4], considering an AWGN channel.

A performance analysis of the 16APSK and the 32APSK modulations for DVB-S2 transmissions over nonlinear channels is made in [6]. The amplifier nonlinearity is modeled according to a soft-limiter and to a TWTA. Analytical performance expressions are derived taking into account a one-link communication channel.

In [7], the performance of pre-distorted APSK modulations for one-link and two-link nonlinear satellite communication channels is addressed. However, the up-link noise is disregarded, limiting the scope of the results to a one-link channel or to a two-link channel under very high signal-to-noise ratio (SNR) in the up-link.

### B. Contributions and organization of the article

In this paper, the 2r16APSK modulation is contrasted with the DVB-S2 16APSK modulation aiming at verifying if the 2r16APSK can be considered an alternative choice for DVB-S2 and other similar communication systems in the presence of nonlinear distortion. To this end, the performances of both modulations are assessed in terms of bit error rate (BER), constellation figure of merit (CFM), peak-to-average power ratio (PAPR), total degradation (TD) versus input back-off (IBO), and spectral regrowth, when the transmitted signal goes through a complete two-link satellite channel (with noise in both links) under nonlinear AM-to-AM and AM-to-PM distortions produced by a TWTA, which is simulated under the Saleh model [8].

Besides the above contribution, the paper also uncovers important hints on the modeling and simulation aspects of a two-link satellite channel, mainly in what concerns the noise calibration for fair analyses, the signal and distortion modeling and realization, and the receiver calibration for coherent detection of a distorted constellation without transmitted signal pre-distortion.

The other sections of this paper are organized as follows: The rules for constructing the 2r16APSK and the 16APSK constellations are described in Section II. Section III is devoted to the system model adopted to access the performance of the 2r16APSK and the 16APSK modulations when operating over a two-link nonlinear satellite channel. The metrics adopted in the performance assessment are described in Section IV. Numerical results and discussions are given in Section V, and the conclusions are drawn in Section VI.

## II. 2R16APSK AND DVB-S2 16APSK CONSTELLATIONS

The 2r16APSK constellation can be generated as follows [4]: Let the  $i$ -th unit-energy signal-vector (constellation symbol) of a 16PSK modulation,  $i = 1, \dots, 16$ , be written as

$$\mathbf{u}_i = \begin{bmatrix} \cos [(i-1)\pi/8] \\ \sin [(i-1)\pi/8] \end{bmatrix}. \quad (1)$$

For  $k = 1, \dots, 8$ , let

$$\mathbf{u}_{2k} \leftarrow 1.612\mathbf{u}_{2k}, \quad (2)$$

which is made to move 8 out of the 16 symbols to the outer ring, where 1.612 is the optimal radius ratio determined in [4].

Finally, the 2r16APSK symbols with average energy  $E$  are given by

$$\mathbf{s}_i = \frac{\mathbf{u}_i\sqrt{E}}{\sqrt{\frac{1}{16}\sum_{k=1}^{16}\mathbf{u}_k^T\mathbf{u}_k}}, \quad (3)$$

where  $[\cdot]^T$  denotes vector transposition, and where it is implicitly assumed that symbols are equally likely.

The symbols of the 16APSK constellation can be generated as follows: For  $j = 1, \dots, 4$ , let

$$\mathbf{w}_j = \begin{bmatrix} \cos [(2j-3)\pi/4]/\gamma \\ \sin [(2j-3)\pi/4]/\gamma \end{bmatrix}, \quad (4)$$

where  $\gamma$  is from [5, Table 9], defining the radius ratio of the symbol rings. For  $k = 1, \dots, 12$ , let

$$\mathbf{w}_k = \begin{bmatrix} \cos [(2k-3)\pi/12] \\ \sin [(2k-3)\pi/12] \end{bmatrix}. \quad (5)$$

For  $i = 1, 2, \dots, 16$ , then the 16APSK signal-vectors are

$$\mathbf{s}_i = \begin{cases} \mathbf{w}_i, & \text{for } i \leq 12 \\ \mathbf{u}_{i-12}, & \text{otherwise} \end{cases}. \quad (6)$$

Also assuming equally likely symbols, the 16APSK signal-vectors with average energy  $E$  become

$$\mathbf{s}_i \leftarrow \frac{\mathbf{s}_i\sqrt{E}}{\sqrt{\frac{1}{16}\sum_{k=1}^{16}\mathbf{s}_k^T\mathbf{s}_k}}. \quad (7)$$

The resultant 2r16APSK and 16APSK constellations, along with their bit labeling, are illustrated in Fig. 1.

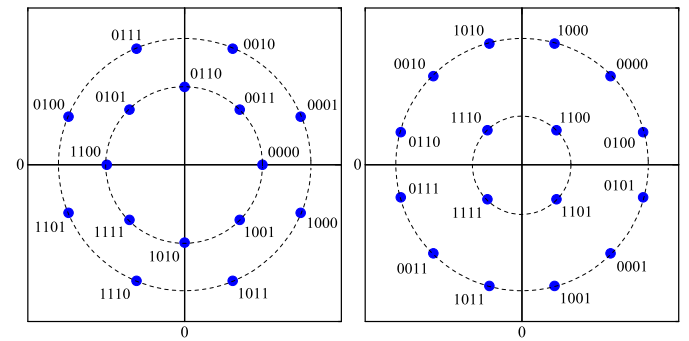


Fig. 1. 2r16APSK constellation (left) and DVB-S2 16APSK constellation for  $\gamma = 2.57$  (right), and their bit labeling [4], [5].

## III. SYSTEM MODEL

The vector model of a two-link fixed satellite communication system from the perspective of performance analysis via computer simulations is shown in Fig. 2. The input data bits are mapped into the constellation signal-vectors, which subsequently generate the modulated signal in complex envelope representation.

The transmitted complex symbols are impaired by an up-link complex additive white Gaussian noise, and then nonlinearly amplified to be transmitted in the down-link channel.

At the receiver, the down-link complex additive white Gaussian noise is added. The corrupted received symbols go through the detection process, where symbol estimation is made. Each estimated symbol is subsequently mapped back into the data bits that it represents<sup>1</sup>.

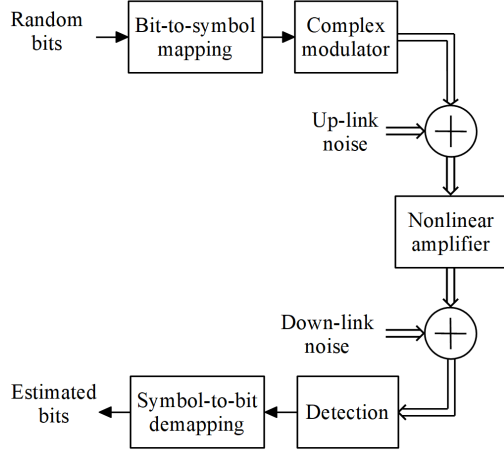


Fig. 2. Model of a two-link satellite communication system [7], [10], [11].

The  $i$ -th signal-vector of the 2r16APSK and the 16APSK constellations, for  $i = 1, \dots, 16$ , can be written as

$$\mathbf{s}_i = \begin{bmatrix} s_{i1} \\ s_{i2} \end{bmatrix}. \quad (8)$$

Additionally, according to [12, Ch. 5], the  $i$ -th passband symbol can be described by

$$s_i(t) = s_{i1} \sqrt{\frac{2}{T}} \cos(2\pi f_c t) + s_{i2} \sqrt{\frac{2}{T}} \sin(2\pi f_c t), \quad (9)$$

where  $T$  is the symbol duration, in seconds, and  $f_c$  is the carrier frequency, in Hertz.

The  $i$ -th passband symbol can be also written using the complex envelope [13] symbol representation

$$\tilde{s}_i(t) = s_I(t) + j s_Q(t), \quad (10)$$

from where the passband symbol can be written according to

$$s_i(t) = s_I(t) \cos(2\pi f_c t) - s_Q(t) \sin(2\pi f_c t). \quad (11)$$

During a given symbol interval  $(t, t+T]$ , assuming without loss of generality that  $T = 2$ , it follows from (9) and (11) that the in-phase and the quadrature components of the complex transmitted symbols  $\tilde{s}_i(t)$  are respectively  $s_I(t) = s_{i1}$  and  $s_Q(t) = -s_{i2}$ , yielding

$$\tilde{s}_i(t) = s_{i1} - j s_{i2}. \quad (12)$$

<sup>1</sup>The present model suits to a geostationary orbit (GEO) satellite and a fixed receiver. If a mobile receiver is considered, fading and shadowing effect must be inserted into the down-link path, before noise addition [9].

Thus, to model the complex envelope of the transmitted symbols, it suffices to represent them into the signal-vector form given in (8), with coordinates  $s_{i1}$  and  $-s_{i2}$ .

The transmitted symbol signal-vectors are added to a two-dimensional zero-mean Gaussian noise vector in the up-link. The variance of this noise is

$$\sigma_u^2 = \frac{N_0}{4G_p}, \quad (13)$$

where  $N_0$  is the noise power spectral density, in watts per Hertz, and  $G_p$  is the dimensionless power gain of the satellite's nonlinear amplifier, whose calculation is given a little ahead, after the nonlinear amplifier model is described.

The amplified up-link noise variance is half of the total (up-link plus down-link) noise variance  $\sigma^2 = N_0/2$ . Hence, the variance of the down-link noise is

$$\sigma_d^2 = \frac{N_0}{4}. \quad (14)$$

Considering that the amplifier nonlinearity is memoryless, it can be described by the widely-accepted Saleh model [8], in which the AM-to-AM and AM-to-PM transfer functions of a typical TWTA are expressed as

$$A(r) = \frac{\alpha_a r}{1 + \beta_a r^2} \quad (15)$$

and

$$\Phi(r) = \frac{\alpha_\phi r^2}{1 + \beta_\phi r^2}, \quad (16)$$

respectively, where  $r$  is the input signal magnitude normalized to its corresponding value at the saturation point of the amplifier, and the parameters  $\alpha_a = 2.1587$ ,  $\beta_a = 1.1517$ ,  $\alpha_\phi = 4.0033$  and  $\beta_\phi = 9.1040$  are those determined by curve-fitting using actual TWTA data, as reported in [8].

The transfer functions (15) and (16) are plotted in Fig. 3, along with the input back-off (IBO) and the output back-off (OBO) that are associated to the operating point of the TWTA.

The IBO is the difference, in dB, between the actual input amplitude (or power) and the input amplitude (or power) necessary for saturating the amplifier. The OBO is the difference, in dB, between the output amplitude (or power) and the output amplitude (or power) at the saturation, which is the maximum output amplitude (or power) of the amplifier.

The IBO, in dB, can be calculated as

$$\text{IBO} = -20 \log_{10}(\sqrt{E}), \quad (17)$$

where  $E$  is the average symbol energy of the input constellation. Obviously, the IBO can be calculated by replacing  $E$  by the average signal power.

In light of (15), it is easy to verify that the OBO, in dB, can be calculated as a function of the IBO according to

$$\text{OBO} = -20 \log_{10} \left[ \frac{\alpha_a 10^{-\frac{\text{IBO}}{20}}}{1 + \beta_a \left( 10^{-\frac{\text{IBO}}{20}} \right)^2} \right]. \quad (18)$$

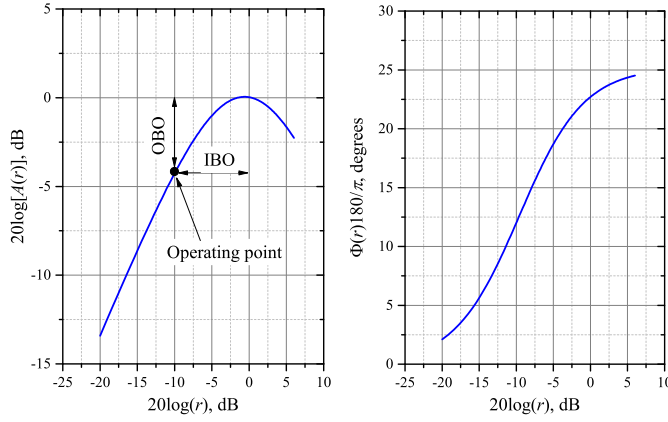


Fig. 3. AM-to-AM (left) and AM-to-PM (right) transfer functions of a TWTA. The operating point defined by the input back-off (IBO) and the output back-off (OBO) is highlighted in the graph on the left.

Assuming no pre-distortion applied at the transmitter (Earth station) side, the distorted signal-vectors at the output of the TWTA become

$$\mathbf{s}_i \leftarrow \begin{bmatrix} \frac{\alpha_a |\mathbf{s}_i|}{1 + \beta_a |\mathbf{s}_i|^2} \cos \left[ \frac{\alpha_\phi |\mathbf{s}_i|^2}{1 + \beta_\phi |\mathbf{s}_i|^2} + \arg(\mathbf{s}_i) \right] \\ -\frac{\alpha_a |\mathbf{s}_i|}{1 + \beta_a |\mathbf{s}_i|^2} \sin \left[ \frac{\alpha_\phi |\mathbf{s}_i|^2}{1 + \beta_\phi |\mathbf{s}_i|^2} + \arg(\mathbf{s}_i) \right] \end{bmatrix}, \quad (19)$$

where  $|\mathbf{s}_i|$  and  $\arg(\mathbf{s}_i)$  denote the modulus and the phase of  $\tilde{\mathbf{s}}_i(t)$  defined in (12), in polar form.

Fig. 4 shows an undistorted and a distorted 2r16APSK constellation, with the distorted constellation generated from the coordinates given in (19), which were generated from the undistorted signal-vectors obtained from (1), (2) and (3). From this figure it can be noticed the amplitude-dependent compression of the constellation caused by the AM-to-AM transfer characteristic, and the amplitude-dependent phase rotation caused by the AM-to-PM transfer characteristic.

Now, the power gain  $G_p$  in (13) can be properly defined as the ratio between the average symbol energies of the distorted and the undistorted constellations, that is,

$$G_p = \frac{1}{16E} \sum_{i=1}^{16} \left[ \frac{\alpha_a |\mathbf{s}_i|}{1 + \beta_a |\mathbf{s}_i|^2} \right]^2, \quad (20)$$

where  $\mathbf{s}_i$  comes from (19).

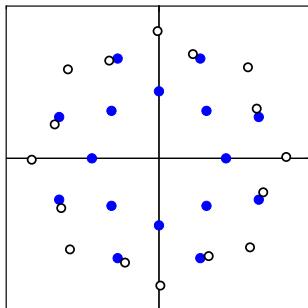


Fig. 4. Undistorted (filled dots) and nonlinearly amplified (unfilled dots) 2r16APSK constellation.

At the receiver side in Fig. 2, a maximum-likelihood (ML) detection process estimates the transmitted symbol  $\hat{\mathbf{s}}_i$  as the one closest, in terms of Euclidean distance, to the received signal-signal vector  $\mathbf{x}$ , that is,

$$\hat{\mathbf{s}}_i = \min_i \|\mathbf{x} - \mathbf{s}_i\|, \quad (21)$$

where  $\mathbf{s}_i$  belongs to the reference constellation in use, which can be modified to take into account the AM-to-AM and AM-to-PM distortions. The AM-to-AM and AM-to-PM distortions can be accounted for by means of pre-distortion at the transmitter side, with the objective of restoring the shape of the original constellation after nonlinear amplification, or by means of adopting a modified reference constellation, for detection purposes, at the receiver side.

A simple constellation pre-distortion strategy is adopted in [7], where the radius of the outer circle and the phase shift for each circle are adjusted to obtain a close approximation to the undistorted signal constellation after nonlinear amplification. This adjustment is made by hand in [7], assuming knowledge of the TWTA transfer characteristics.

Here, an even simpler method is adopted, in which a modified reference constellation at the receiver is used, assuming no knowledge of the TWTA transfer characteristics. It makes use of the inherent carrier recovery effect when coherent detection takes place: the received constellation is rotated back to its original reference position, which is equivalent of rotating the constellation in the same amount of the rotation produced by the channel, but in the opposite direction. In terms of modeling for simulation purposes, the reference constellation is formed by rotating the original constellation in an amount

$$\bar{\phi} = \frac{1}{2} \left( \frac{\alpha_\phi |\mathbf{s}_i^i|^2}{1 + \beta_\phi |\mathbf{s}_i^i|^2} + \frac{\alpha_\phi |\mathbf{s}_i^o|^2}{1 + \beta_\phi |\mathbf{s}_i^o|^2} \right), \quad (22)$$

where the two terms between parentheses are the rotations produced by the TWTA in any of the symbols belonging to the inner (superscript  $i$ ) and outer (superscript  $o$ ) constellation rings. Thus,  $\bar{\phi}$  is the average of the rotations produced in the inner and outer symbols. Hence, the reference constellation symbols for ML detection become

$$\mathbf{s}_i \leftarrow \sqrt{G_p} \begin{bmatrix} |\mathbf{s}_i| \cos [\arg(\mathbf{s}_i) + \bar{\phi}] \\ -|\mathbf{s}_i| \sin [\arg(\mathbf{s}_i) + \bar{\phi}] \end{bmatrix}, \quad (23)$$

where the multiplication by  $\sqrt{G_p}$  equates the reference and the received constellations' energies, which in practice is accomplished by the receiver's automatic gain control (AGC).

An alternative way of modifying the reference constellation at the receiver is to distort it according to the TWTA transfer functions, which obviously demands the knowledge of these functions in advance. This alternative represents an opportunity to be investigated.

#### IV. PERFORMANCE METRICS

This section briefly describes some metrics that can be adopted to assess the performance of any digital modulation over a two-link satellite channel. The 2r16APSK and the DVB-S2 16APSK modulations are compared using all of them.

*A. Bit error probability,  $P_b$*

The bit error probability,  $P_b$ , or its estimate, the BER, is obviously of paramount importance to assess the communication system performance, since it indirectly measures the intelligibility of the information delivered to the destination.

However, the mathematical tractability of the system depicted in Fig. 2 for theoretical calculation of  $P_b$  is quite intricate due to the up-link noise portion that appears at the detector input affected by the nonlinearity of the satellite's amplifier. The determination of the distribution of this noise is the main cause of the mathematical intractability [11, p. 7]. In other words, both the up-link and the down-link noises are Gaussian, but the up-link noise is affected by the amplifier nonlinearity before added to the down-link noise, yielding a composite noise that is no longer Gaussian at the destination receiver. In this scenario, a computer simulation is the safer choice to estimate  $P_b$  by means of the BER.

On the other hand, the  $P_b$  related to the non-distorted constellation (pure AWGN channel) can be theoretically determined, and the union bound [14, p. 772] is used here for this purpose. The union bound on  $P_b$  for a digital modulation over the AWGN channel can be obtained from the constellation geometry and the symbol-to-bit mapping rule, and is given by

$$P_b \leq \frac{1}{2M \log_2 M} \sum_{i=1}^M \sum_{\substack{k=1 \\ k \neq i}}^M d_{i,k}^H \operatorname{erfc} \left( \frac{d_{i,k}^E}{2\sqrt{N_0}} \right), \quad (24)$$

where  $M$  is the number of symbols,  $d_{i,k}^E = \|\mathbf{s}_i - \mathbf{s}_k\|$  is the Euclidean distance between  $\mathbf{s}_i$  and  $\mathbf{s}_k$ , with  $\|\cdot\|$  denoting the Euclidean norm, and  $d_{i,k}^H$  is the Hamming distance between the binary words into which  $\mathbf{s}_i$  and  $\mathbf{s}_k$  are mapped.

Although (24) is an upper bound, it is known to closely approximate the actual  $P_b$  for moderate-to-high SNR regimes. The approximation also occurs in low SNRs if only the nearest neighbor symbols are considered in the computation of the conditional symbol errors implicit in (24).

After  $P_b$  is determined from (24), it is usual to express  $d_{i,k}^E$  as a function of the average energy per bit,  $E_b$ , eventually having an expression of  $P_b$  as a function of the average SNR per bit,  $E_b/N_0$ .

It is noteworthy that the union bound cannot be applied to compute the bit error probability of the two-link satellite communication system. This is because both the up-link and the down-link noises are Gaussian, but the up-link noise is affected by the amplifier nonlinearity before added to the down-link noise, yielding a composite noise that is no longer Gaussian at the destination receiver. Hence, as already mentioned, a computer simulation is the safer method to estimate  $P_b$  when nonlinear transfer functions are on the noise path.

*B. Constellation figure of merit, CFM*

The CFM, which is an indirect measure of the modulation power efficiency [15], is the quotient between the squared minimum Euclidean distance between any pair of constellation symbols and the average constellation energy, that is,  $\text{CFM} = d_{\min}^2/E$ . Thus, a higher CFM is expected to correspond to a higher power efficiency, i.e., a lower bit error probability.

Meanwhile it remains unclear if the CFM value is indeed consistent with the bit error probability of a modulation for the whole range of  $E_b/N_0$  of interest. The numerical results in Section V helps clarifying this matter.

*C. Peak-to-average power ratio, PAPR*

As the name suggests, the PAPR is the ratio between the peak and the average power of a signal. A high PAPR signal is amplified with less power efficiency, since its power needs to be reduced to avoid severe distortion to the signal peaks. Moreover, a high PAPR signal is more prone to the spectral regrowth caused by intermodulation when the signal is nonlinearly amplified [12, p. 511, 529], [16].

The transmitted signal PAPR does not only depend on the constellation geometry, but also on the characteristics of the transmitter's pulse shaping filter. Assuming the use of a root raised cosine (RRC) filter, it has been found in [4], [17] that the minimum PAPR occurs around a filter roll-off of 0.5, increasing slightly above this value. Below 0.5, the PAPR increases in a more pronounced way.

Remarkably, it has been found that the PAPR computed using the maximum symbol energy,  $E_{\max}$ , and the average symbol energy,  $E$ , both considering the undistorted constellation, is approximately the same as the one computed with an RRC-filtered signal for a roll-off equal to 0.5. Hence, from a theoretical perspective, it follows that

$$\text{PAPR} = 10 \log_{10} \left( \frac{2E_{\max}}{E} \right). \quad (25)$$

*D. Total degradation, TD*

The  $P_b$  and the CFM seem sufficient and equivalent performance metrics when the modulated signal goes through a linear channel. However, in the case of the two-link satellite communication channel considered in this paper, these metrics may lead to incorrect conclusions, and the adoption of a more adequate metric is made necessary.

The PAPR seems to be useful, but the total degradation has been unveiled even more meaningful from a practical standpoint [6]. The total degradation, in dB, is defined as

$$\text{TD} = \Delta_{\text{SNR}} + \text{OBO}, \quad (26)$$

where  $\Delta_{\text{SNR}}$  is the SNR difference, in dB, required to attain a given reference bit or symbol error rate, with and without the effect of nonlinearity [6].

The TD not only takes into account the necessary increment made in the SNR to achieve the same error rate of the undistorted constellation, but also the OBO that results from a given IBO at the target error rate. Thus, the optimal amplifier's operating point is determined from the IBO associated to the minimum attainable value of TD.

The computation of TD needs to be made via computer simulation due to the difficulty in finding  $\Delta_{\text{SNR}}$  analytically, which would need a formula for the bit or symbol error rate under the two-link satellite communication model depicted in Fig. 2, as highlighted in Section IV-A.



E. Spectral regrowth

Spectral regrowth is the spectral broadening caused by intermodulation when the signal goes through a nonlinear device [11, p. 744], [12, p. 511, 529], [16]. Normally, the amount of spectral regrowth is directly proportional to the PAPR of the signal at the input of the nonlinear device, which in turn depends on the characteristics of the filter applied to the signal before nonlinear distortion. For example, the influence of the roll-off of an RRC filter on the PAPR is analyzed in [17].

Spectral regrowth may cause adjacent channel interference, requiring additional filtering after amplification, which may be costly due to the high power of the signal to be filtered.

V. NUMERICAL RESULTS

Due to the nonexistence of accurate expressions for a complete theoretical performance analysis of the two-link satellite communication system, owed mainly to the nonlinearly distorted up-link noise that appears at the detector input, the results shown hereafter were obtained by Monte Carlo computer simulation.

To check if the simulation is properly calibrated, one may plot the union bound (24) applied to the distorted constellation, against the BER estimated via maximum-likelihood detection referenced to the distorted constellation in terms of symbol positions and average symbol energy. The up-link noise must be zeroed, that is,  $\sigma_u^2 = 0$  and  $\sigma_d^2 = \sigma^2 = N_0/2$ . This check has been made before the results reported in this section were obtained.

Fig. 5 shows the PAPR of the modulations in analysis, as a function of the roll-off of the RRC filter used to shape the modulated signal symbols. The results were obtained with the help of a simulation implemented in VisSim/Comm [18], which is a software tool for modeling and simulating dynamic systems. From this figure it can be seen that the 16APSK modulations have approximately the same PAPR values, with a slight advantage of the 16APSK with  $\gamma = 2.57$ . The 2r16APSK modulation has a PAPR around 1 dB worse than the ones achieved with the 16APSK modulations for a roll-off around 0.5. The PAPR differences become a little smaller at lower roll-offs, and a little larger at higher roll-offs.

Denoting the smallest and the largest constellation radius as  $R_1$  and  $R_2$ , respectively, for the 2r16APSK it follows from (2) or from [4] that  $\gamma = R_2/R_1 = 1.612$ . Then, the average symbol energy is  $E = (8R_1^2 + 8R_2^2)/16 = (R_1^2 + R_2^2)/2$ , yielding  $R_2^2 = E_{max} = 2E/(1/\gamma^2 + 1)$ . Plugging this result into (25) one obtains  $PAPR = 4.6066$  dB.

In the case of the 16APSK, it follows that  $E = (4R_1^2 + 12R_2^2)/16 = (R_1^2 + 3R_2^2)/4$ , yielding  $R_2^2 = E_{max} = 4E/(1/\gamma^2 + 3)$ . Plugging this result into (25) yields  $PAPR = 4.0459$  dB for  $\gamma = 2.57$ , and  $PAPR = 4.1162$  dB for  $\gamma = 3.15$ .

From these PAPR values it can be concluded, at least in a first look, that the 16APSK modulation will perform better under nonlinear distortion than the 2r16APSK modulation, with an advantage in the use of  $\gamma = 2.57$  over  $\gamma = 3.15$  in the case of the 16APSK modulations. This conclusion will be contrasted with those obtained from other metrics.

Comparing the PAPR values reported in the previous paragraphs with those obtained from Fig. 5, it is verified that the

PAPR calculated using (25) indeed matches the one computed with an RRC-filtered signal for a roll-off equal to 0.5.

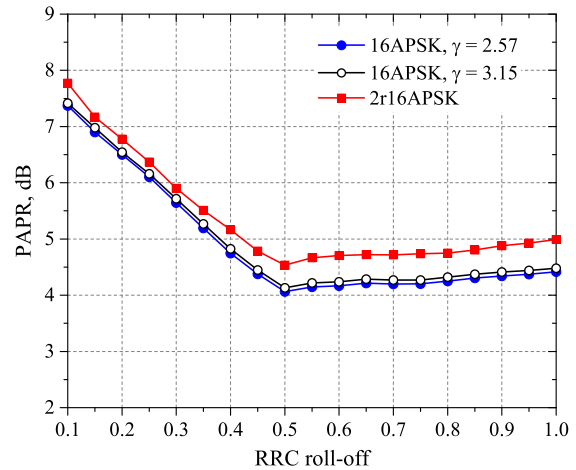


Fig. 5. Peak-to-average power ratio of RRC-filtered 2r16APSK, 16APSK with  $\gamma = 2.57$ , and 16APSK with  $\gamma = 3.15$ .

Fig. 6 shows the bit error rates of distorted and undistorted constellations 2r16APSK, 16APSK with  $\gamma = 2.57$ , and 16APSK with  $\gamma = 3.15$ . The theoretical bit error probabilities computed via the union bound (24) are also shown in the case of undistorted constellations, considering only the errors to the nearest-neighbor symbols.

When no distortion is present, it can be seen in Fig. 6 that the performances of all modulations are quite close to each other for the whole range of  $E_b/N_0$  shown. As  $E_b/N_0$  increases, it can be observed that the modulation 16APSK with  $\gamma = 2.57$  becomes the most power-efficient, followed by the 2r16APSK, and then by the 16APSK with  $\gamma = 3.15$ .

If nonlinear distortion takes place, it can be noticed from Fig. 6 that the 16APSK modulation with  $\gamma = 3.15$  becomes the most power-efficient, followed by the 2r16APSK, and then by the 16APSK with  $\gamma = 2.57$ . The performance differences among them increase considerably as  $E_b/N_0$  is increased.

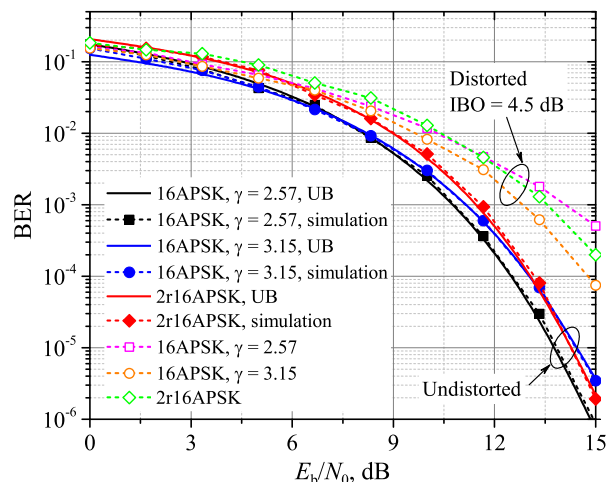


Fig. 6. Bit error rate of distorted and undistorted 2r16APSK, 16APSK with  $\gamma = 2.57$ , and 16APSK with  $\gamma = 3.15$ .

Contrasting the metrics BER and CFM, from [4] it can be obtained that the minimum Euclidean distance between any pair of symbols in the 2r16APSK constellation is  $d_{\min} = [4E(1 - \sqrt{2}/2)/3.6]^{1/2}$ . Hence, it follows that  $\text{CFM} = 0.3254$ .

Based on the 16APSK constellation geometry analyzed in [6], it can be found that  $d_{\min} = 4 \sin(\pi/12) [E/(3+1/\gamma^2)]^{1/2}$  for  $\gamma = 2.57$ , and  $d_{\min} = [8E/(1+3\gamma^2)]^{1/2}$  for  $\gamma = 3.15$ , where these values of  $\gamma$  are the smallest and the largest values given in [5, Table 9], which are the ones chosen for analysis herein, since they represent the extreme cases. Thus, the constellation figure of merit are  $\text{CFM} = [16\gamma^2 \sin^2(\pi/12)/(1+3\gamma^2)] = 0.3401$  and  $\text{CFM} = 8/(1+3\gamma^2) = 0.2600$ , respectively.

Hence, the 16APSK modulation with  $\gamma = 2.57$  is the more power-efficient ( $\text{CFM} = 0.3401$ ), which is closely followed by the 2r16APSK ( $\text{CFM} = 0.3254$ ), which is then followed by the 16APSK with  $\gamma = 3.15$  ( $\text{CFM} = 0.2600$ ). Notice that the bit error probability results presented in Fig. 6 are consistent with this CFM rank, considering an undistorted constellation, but only under a high SNR regime.

Fig. 7 shows the power spectral densities (PSDs) of the modulated complex envelope signal at the input and at the output of the TWTA. The frequency axis is normalized with respect to the symbol rate. The figure only shows the PSDs of the 2r16APSK signal, since approximately equal PSDs have been observed for all modulations in analysis; the other results were omitted for conciseness.

Although the spectral regrowth is directly proportional to the PAPR of the signal at the input of the nonlinear device, the PAPR differences observed in Fig. 5 were not capable of producing noticeable differences among the analyzed modulations in terms of the spectral regrowth.

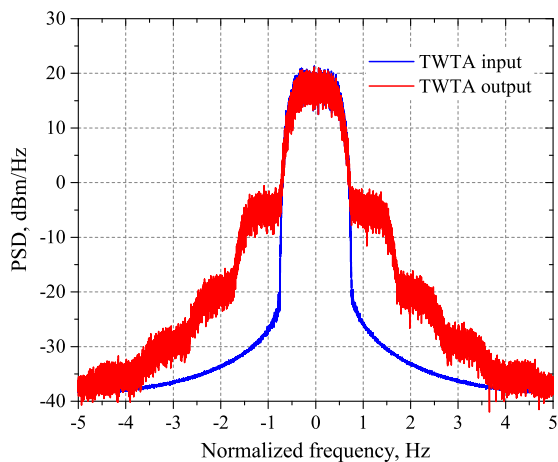


Fig. 7. Spectral regrowth of the 2r16APSK, 16APSK with  $\gamma = 2.57$ , and 16APSK with  $\gamma = 3.15$  RRC-filtered signals, with a roll-off of 0.5. The IBO is 4.5 dB, and the TWTA parameters are those given in [8].

Aiming at compensating for poor usefulness of the previous metrics in some circumstances, or possible inconsistencies among them, the total degradation metric defined in (26) is analyzed in what follows.

Fig. 8 gives the TD experienced by the modulations under assessment, for a reference bit error probability of  $1 \times 10^{-3}$ .

Two cases are considered: A) full distortion according to the Saleh model with  $\alpha_a = 2.1587$ ,  $\beta_a = 1.1517$ ,  $\alpha_\phi = 4.0033$  and  $\beta_\phi = 9.1040$ , which corresponds to a TWTA; B) no phase distortion ( $\alpha_\phi = 0$ ), which better suits to model a SSPA.

From Fig. 8 it can be seen that the smallest degradation,  $\text{TD}_{\min} \approx 2.5$  dB is achieved by the 16APSK modulation with  $\gamma = 3.15$  under Case A, yielding an optimum input back-off  $\text{IBO}_{\text{opt}} \approx 5$  dB. The 2r16APSK modulation comes in the second position, achieving  $\text{TD}_{\min} \approx 2.75$  dB at  $\text{IBO}_{\text{opt}} \approx 5$  dB. The 16APSK modulation with  $\gamma = 2.57$  occupies the third position, achieving  $\text{TD}_{\min} \approx 3.5$  dB at  $\text{IBO}_{\text{opt}} \approx 6$  dB.

Under Case B, the same rank is observed in Fig. 8, with the results:  $\text{TD}_{\min} \approx 1.7$  dB at  $\text{IBO}_{\text{opt}} \approx 5$  dB for the 16APSK modulation with  $\gamma = 3.15$ ,  $\text{TD}_{\min} \approx 2.4$  dB at  $\text{IBO}_{\text{opt}} \approx 5$  dB for the 2r16APSK modulation, and  $\text{TD}_{\min} \approx 2.9$  dB at  $\text{IBO}_{\text{opt}} \approx 6$  dB for the 16APSK modulation with  $\gamma = 2.57$ .

From all results presented in this section, it can be concluded that the 2r16APSK modulation lies in-between the two 16APSK modulations adopted in the DVB-S2 standard in terms of the most relevant performance metrics considered herein.

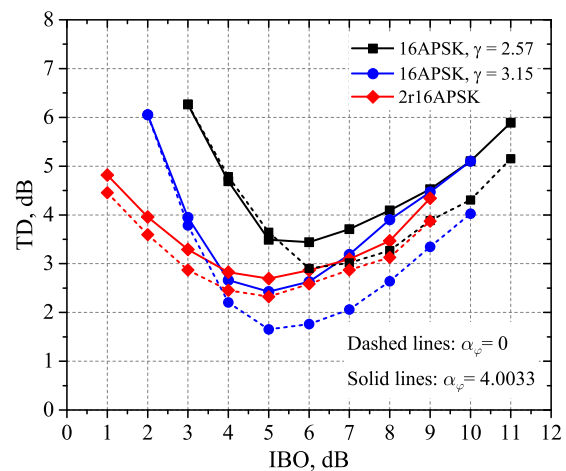


Fig. 8. Total degradation of 2r16APSK, 16APSK with  $\gamma = 2.57$ , and 16APSK with  $\gamma = 3.15$ . The remaining TWTA parameters are  $\alpha_a = 2.1587$ ,  $\beta_a = 1.1517$ , and  $\beta_\phi = 9.1040$ .

## VI. CONCLUSIONS

In this paper, the 2r16APSK modulation were contrasted with the 16APSK modulation adopted by the DVB-S2 standard, under the nonlinear distortion present in a two-link satellite channel, using several performance metrics. In the case of undistorted received signal, the bit error probability and the constellation figure of merit have shown to be consistent with each other under a high signal-to-noise ratio regime. This consistency is lost when nonlinear distortion takes place. In this case, the spectral regrowth lacks from accuracy, and the peak-to-average power ratio and the bit error probability are inconsistent, which renders the total distortion a more adequate performance metric. The overall analysis of the results demonstrated that the 2r16APSK is indeed an adequate alternative choice for the DVB-S2 and other alike communication systems subjected to nonlinear distortions.

## REFERENCES

- [1] B. R. Elbert, *Introduction to Satellite Communication*, 3rd ed. Boston, USA: Artech House, 2008. [Online]. Available: <https://us.artechhouse.com/Introduction-to-Satellite-Communication-Third-Edition-P1736.aspx>
- [2] C. Paoloni, D. Gamzina, R. Letizia, Y. Zheng, and N. C. L. Jr., "Millimeter wave traveling wave tubes for the 21st century," *Journal of Electromagnetic Waves and Applications*, vol. 35, no. 5, pp. 567–603, 2021, doi: 10.1080/09205071.2020.1848643.
- [3] C. Thomas, M. Weidner, and S. Durrani, "Digital amplitude-phase keying with M-ary alphabets," *IEEE Trans. Commun.*, vol. 22, no. 2, pp. 168–180, February 1974, doi: 10.1109/TCOM.1974.1092165.
- [4] D. A. Guimarães, "Two-radii 8APSK and two-radii 16APSK modulations as alternatives to 8PSK and 16QAM," *Journal of Communication and Information Systems*, vol. 33, no. 1, Sep. 2018, doi: 10.14209/jcis.2018.30. [Online]. Available: <https://jcis.sbrrt.org.br/jcis/article/view/574>
- [5] European Telecommunications Standards Institute (ETSI), "Digital video broadcasting (DVB); second generation framing structure, channel coding and modulation systems for broadcasting, interactive services, news gathering and other broadband satellite applications (DVB-S2)," March 2013. [Online]. Available: [http://www.etsi.org/deliver/etsi\\_en/302300\\_302399/302307/01.03.01\\_60/en\\_302307v010301p.pdf](http://www.etsi.org/deliver/etsi_en/302300_302399/302307/01.03.01_60/en_302307v010301p.pdf).
- [6] W. Sung, S. Kang, P. Kim, D.-I. Chang, and D.-J. Shin, "Performance analysis of APSK modulation for DVB-S2 transmission over nonlinear channels," *Int. J. Satellite Communications Networking*, vol. 27, pp. 295–311, 2009, doi: 10.1002/sat.938.
- [7] Y. Zhou, P. McLane, and C. Loo, "Performance of predistorted APK modulation for one- and two-link nonlinear power amplifier satellite communication channels," *IEEE Trans. Veh. Technol.*, vol. 54, no. 2, pp. 629–638, 2005, doi: 10.1109/TVT.2004.841539.
- [8] A. Saleh, "Frequency-independent and frequency-dependent nonlinear models of twt amplifiers," *IEEE Trans. Commun.*, vol. 29, no. 11, pp. 1715–1720, 1981, doi: 10.1109/TCOM.1981.1094911.
- [9] M. Tropea and F. De Rango, "A comprehensive review of channel modeling for land mobile satellite communications," *Electronics*, vol. 11, no. 5, 2022, doi: 10.3390/electronics11050820.
- [10] M. C. Jeruchim, P. Balaban, and K. S. Shanmugan, *Simulation of Communication Systems: Modeling, Methodology and Techniques*, 2nd ed. USA: Kluwer Academic Publishers, 2006. [Online]. Available: <https://books.google.fr/books?id=K1wKBwAAQBAJ>
- [11] W. Tranter, K. Shanmugan, T. Rappaport, and K. Kosbar, *Principles of Communication Systems Simulation with Wireless Applications*. USA: Prentice Hall, 2003. [Online]. Available: <https://dl.acm.org/doi/10.5555/1407789>
- [12] D. A. Guimarães, *Digital Transmission: A Simulation-Aided Introduction with VisSim/Comm*, ser. Signals and Communication Technology. Springer, 2009, doi: 10.1007/978-3-642-01359-1.
- [13] D. A. Guimarães, "Complex envelope based modems: A tutorial," *Journal of Communication and Information Systems*, vol. 35, no. 1, pp. 34–50, Feb. 2020, doi: 10.14209/jcis.2020.4. [Online]. Available: <https://jcis.sbrrt.org.br/jcis/article/view/689>
- [14] M. Simon and M. Alouini, *Digital Communication over Fading Channels*, ser. Wiley Series in Telecommunications and Signal Processing. Wiley, 2005, doi: 10.1002/0471715220.
- [15] G. D. Forney and L.-F. Wei, "Multidimensional constellations. I. introduction, figures of merit, and generalized cross constellations," *IEEE Journal on Selected Areas in Communications*, vol. 7, no. 6, pp. 877–892, Aug 1989, doi: 10.1109/49.29611.
- [16] M. Golio, *The RF and microwave handbook*, 2nd ed. Boca Raton, FL, USA: CRC Press, 2008, doi: 10.1201/9781315217703.
- [17] S. Daumont, B. Rihawi, and Y. Lout, "Root-raised cosine filter influences on PAPR distribution of single carrier signals," in *2008 3rd Int. Symp. on Communications, Control and Signal Processing*, March 2008, pp. 841–845, doi: 10.1109/ISCCSP.2008.4537340.
- [18] Altair Engineering, Inc. (former Visual Solutions, Inc.), "VisSim: A graphical language for simulation and model-based embedded development," Nov. 2015. [Online]. Available: <http://www.vissim.com/products/vissim/comm.html>



**Dayan Adionel Guimarães** received the MSc and the PhD in Electrical Engineering from the State University of Campinas (Unicamp), Brazil, in 1998 and 2003, respectively. He is a Researcher and Senior Lecturer in the National Institute of Telecommunications (Inatel), Brazil. His research focuses the general aspects of wireless communications, specifically radio propagation, digital transmission, dynamic spectrum access, and convex optimization and signal processing applied to telecommunications.